Changes in energy metabolism of *Mycobacterium tuberculosis* in mouse lung and under *in vitro* conditions affecting aerobic respiration

Lanbo Shi*, Charles D. Sohaskey†, Bavesh D. Kana‡, Stephanie Dawes‡, Robert J. North§, Valerie Mizrahi‡, and Maria L. Gennaro*¶

*Public Health Research Institute, Newark, NJ 07103; †Department of Veterans Affairs Medical Center, Long Beach, CA 90822; ‡Centre of Excellence for Biomedical TB Research, University of the Witwatersrand and National Health Laboratory Service, Johannesburg 2000, South Africa; and §Trudeau Institute, Saranac Lake, NY 12983

Communicated by David S. Eisenberg, University of California, Los Angeles, CA, September 9, 2005 (received for review April 15, 2005)

Transcription profiling of genes encoding components of the respiratory chain and the ATP synthesizing apparatus of *Mycobacterium tuberculosis* was conducted *in vivo* in the infected mouse lung, and *in vitro* in bacterial cultures subjected to gradual oxygen depletion and to nitric oxide treatment. Transcript levels changed dramatically as infection progressed from bacterial exponential multiplication (acute infection) to cessation of bacterial growth (chronic infection) in response to host immunity. The proton-pumping type-I NADH dehydrogenase and the *aa3*-type cytochrome *c* oxidase were strongly down-regulated. Concurrently, the less energy-efficient cytochrome *bd* oxidase was transiently up-regulated. The nitrate transporter NarK2 was also up-regulated, indicative of increased nitrate respiration. The reduced efficiency of the respiratory chain was accompanied by decreased expression of ATP synthesis genes. Thus, adaptation of *M. tuberculosis* to host immunity involves three successive respiratory states leading to decreased energy production. Decreased bacterial counts in mice infected with a *cydC* mutant (defective in the cytochrome *bd* oxidase-associated transporter) at the transition to chronic infection provided initial evidence that the *bd* oxidase pathway is required for *M. tuberculosis* adaptation to host immunity. *In vitro*, NO treatment and hypoxia caused a switch from transcription of type I to type II NADH dehydrogenase. Moreover, cytochrome *bd* oxidase expression increased, but cytochrome *c* oxidase expression decreased slightly (nitric oxide) or not at all (hypoxia). These specific differences in respiratory metabolism during *M. tuberculosis* growth arrest *in vitro* and *in vivo* will guide manipulation of *in vitro* conditions to model bacterial adaptation to host immunity.

nitric oxide treatment | transcriptional profiling | dormancy | hypoxia

Mycobacterium tuberculosis is an airborne bacterial pathogen causing a chronic lung infection that passes through several stages. In most infected persons, host defenses either clear infection or drive it into a chronic latent state that is potentially long-lasting. Weakening of host immunity can result in release from latency and reactivation of disease. It has been suggested that various stages of *M. tuberculosis* infection are associated with different physiological states of the pathogen (1–5). Work with murine infection models shows that adaptation of *M. tuberculosis* to host immunity involves replacement of sugars by fatty acids as a carbon and energy source (6, 7). Respiration may also be an important aspect of energy metabolism involved in *M. tuberculosis* adaptation to host immunity, because respiration in bacteria is a flexible process that changes as microorganisms respond to environmental stresses (reviewed in refs. 8 and 9). However it is not known whether bacterial pathogens, including *M. tuberculosis*, reroute electron flow during the infection of a host animal.

One model for studying *M. tuberculosis* adaptation to host immunity involves infecting mice with tubercle bacilli by the respiratory route. The resulting lung infection exhibits both an acute phase (≈20 days of exponential bacterial growth) and a subsequent chronic phase (stabilization of bacterial counts) (10). The latter is thought to result from arrest of bacterial growth (11, 12) caused by expression of host adaptive T helper 1-mediated immunity and the resulting activation of infected macrophages that produce inducible nitric oxide (NO) synthase and consequently NO (reviewed in refs. 13 and 14). NO acts as a potent oxidant and inhibitor of cellular respiration (15, 16). Cultures of *M. tuberculosis* exposed to bacteriostatic concentrations of NO *in vitro* exhibit transcriptional changes, such as the induction of an ≈50-gene set regulated by the *dosS/dosT/dosR* system (17). This regulon (18–20) is also induced in hypoxic cultures undergoing growth arrest (19), following activation of infected macrophages with IFN-γ (21), and upon expression of Th1 immunity in the lungs of infected mice (22). Thus bacterial adaptation to mouse lung immunity shares transcriptional similarities with the bacterial response to agents that modulate cellular respiration, such as NO and hypoxia.

In the present work, we used bacterial transcription profiling to determine whether the transition from acute to chronic infection of the mouse lung entails changes in *M. tuberculosis* respiratory metabolism, and whether *in vitro* exposure of tubercle bacilli to NO or to hypoxia models these changes. *In vivo*, we define a complex transcriptional pattern for *M. tuberculosis* indicative of three successive respiratory states associated with gradually decreasing energy conservation and of a concomitant decreased expression of the ATP synthesizing apparatus. *In vitro*, we find that the response of respiratory metabolism to NO treatment and to hypoxia is also characterized by a transcriptional switch from highly coupled to less energy-efficient pathways, but that differences exist with the situation *in vivo*. Defining the respiratory pathways used by *M. tuberculosis* over the course of infection has had particular relevance to the control of tuberculosis since the discovery of new antitubercular drugs that target respiratory components and ATP synthesis (23–25). Moreover, identifying *in vitro* conditions that adequately model the adaptation of tubercle bacilli to lung immunity facilitates mechanistic investigations of bacterial physiology that are exceedingly difficult to perform in a living animal.

Materials and Methods

Mouse Infection. *M. tuberculosis* strain $H_{37}Rv$ and its mutant derivatives were grown as a suspension culture, as described (26). C57BL/6 mice at 8–10 weeks of age were infected with ≈2×10^2 bacterial colony-forming units (cfu) per mouse, as described

Freely available online through the PNAS open access option.

Abbreviations: NRP, nonreplicating persistence; DETA/NO, 2,2′-(hydroxynitrosohydrazono)bisethanimine; cfu, colony-forming unit.

¶To whom correspondence should be addressed. E-mail: gennaro@phri.org.

(22). At selected times, lungs were harvested from four mice per time point. Enumeration of cfu was obtained by spreading 10-fold serial dilutions of homogenates from half of the lung (attached to the left bronchus) on enriched Middlebrook 7H11 agar (Difco) plates followed by counting bacterial colonies after 3 weeks of incubation at 37°C. The half of the lung attached to the right bronchus was snap-frozen in liquid nitrogen for subsequent RNA extraction.

Gradual Oxygen Depletion *in Vitro*. *M. tuberculosis* $H_{37}Rv$ was grown in liquid culture at 37°C in Dubos Tween-albumin broth (Becton Dickinson), as described (27). Gradual oxygen depletion was obtained by subjecting bacterial cultures to slow magnetic stirring in sealed tubes with a head/space ratio of 0.5 as described (27). At selected times, cells from 2-ml aliquots were harvested by centrifugation and frozen in a dry-ice/alcohol bath for subsequent RNA extraction. Bacterial cfu were enumerated by plating 10-fold serial dilutions of liquid cultures on Dubos oleic albumin agar.

Treatment with Nitric Oxide *in Vitro*. Cultures of *M. tuberculosis* $H_{37}Rv$ were grown at 37°C in Dubos Tween-albumin broth to mid-log phase and treated with increasing concentrations (between 25 and 500 μM) of 2,2′-(hydroxynitrosohydrazono)bisethanimine (DETA/NO) (Sigma). After 30 and 60 min, 4 ml of each culture was centrifuged and the cell pellet frozen in a dry-ice/alcohol bath. Each DETA/NO concentration was tested in triplicate in three independent cultures.

Measurements of Bacterial Transcript Copy Numbers. RNA extraction, RT-PCR, and real-time PCR were performed according to our published protocol (22). Reverse transcription primers, PCR primers, and molecular beacons are listed in Table 2, which is published as supporting information on the PNAS web site. Copy numbers of *M. tuberculosis* 16S rRNA were used as a normalization factor to enumerate bacterial transcripts per cell, because 16S rRNA levels correlate well with cfu during the course of lung infection (22) and during hypoxic incubation (28), regardless of growth stage.

Construction of *cydC* Mutant of *M. tuberculosis*. A *cydC*::*aph* mutant of *M. tuberculosis* $H_{37}Rv$ was constructed by allelic exchange mutagenesis and genotypically confirmed by Southern blot analysis (*Supporting Text*, which is published as supporting information on the PNAS web site). The complementing vector pHTBCYD was constructed by cloning a 6,536-bp EcoRI/EcoRV fragment from pOTBCYD (29) containing 605 bp of DNA upstream of *cydA*, the entire *cydABDC* gene cluster, and 74 bp of DNA downstream of *cydC* in the integrative vector, pHINT. The construct was electroporated into the *cydC*::*aph* mutant strain, and transformants were selected on media containing 50 μg/ml hygromycin.

Results and Discussion

Expression of *M. tuberculosis* Genes Encoding Components of Respiratory Complexes and the ATP Synthesizing Apparatus in the Mouse Lung. Transcriptional profiling was used to identify respiratory pathways used by *M. tuberculosis* during mouse lung infection. Transcript levels were measured for *M. tuberculosis* genes involved in electron flow generated from NADH (Fig. 1). Results for multisubunit enzymes are presented for one representative transcript.

Measurement of bacterial cfu in mouse lungs shows exponential growth for ≈20 days (acute infection) followed by host-immunity-induced stabilization of bacterial counts (chronic infection) (Fig. 2*A*). Normalized transcript copy numbers for *nuoB* (type-I NADH dehydrogenase) and *ctaD* (aa_3-type cytochrome *c* oxidase) decreased from day 12 to day 30 postinfection. This

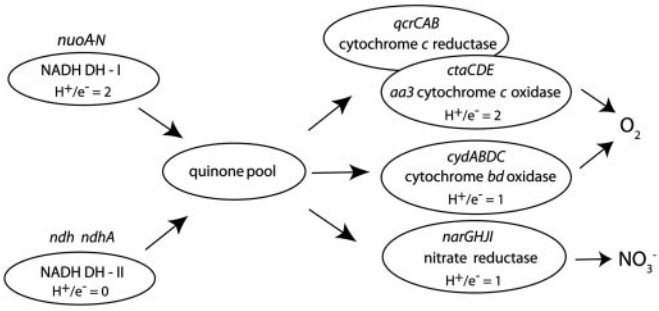

Fig. 1. Architecture of selected respiratory pathways in *M. tuberculosis*. Analysis of the annotated bacterial genome (http://genolist.pasteur.fr/TubercuList) and assignment of putative gene functions based on sequence similarities with other microorganisms suggest that electrons from reducing equivalents generated as NADH by intermediary metabolism are transferred to the membrane-bound menaquinone pool by dehydrogenases. *M. tuberculosis* encodes two types of NADH dehydrogenases (NDH). The type I NDH, encoded by the *nuoA-N* gene cluster, is homologous to the eukaryotic mitochondrial complex, and it couples electron transfer with proton pumping. Two nonproton-pumping type II NDHs, encoded by *ndh* and *ndhA*, also possess NADH/quinol oxidoreductase activity. Reduction of dioxygen is catalyzed by two terminal oxidases: the aa_3-type cytochrome *c* oxidase, encoded by *ctaCDE*, and the *bd*-type menaquinol oxidase, encoded by *cydAB* (the downstream *cydDC* encode an ABC-type transporter). The cytochrome *c* oxidase functions as a proton pump (47), and it likely forms a supercomplex with the cytochrome bc_1 complex (the product of *qcrCAB*), as seen in other actinomycetes such as *Corynebacterium glutamicum* (48). *M. tuberculosis* has the coding potential for utilization of nitrate as alternative electron acceptor (49). Nitrate reduction is associated with the *narGHJI* locus, which encodes nitrate reductase, and *narK2X*, which encodes the nitrate transport protein NarK2 and the ''fused'' inactive nitrate reductase NarX (34).

decrease was 70-fold for *nuoB* and 15-fold for *ctaD* (Fig. 2*B*). Transcript levels for *qcrC* (cytochrome bc_1 complex) and *ndh* (type-II NADH dehydrogenase) decreased slightly during chronic infection (2- to 2.5-fold on day 100 relative to day 15) (Fig. 2*C*). We also measured levels of the *cyd* transcripts. As with other bacteria, the *M. tuberculosis* genome encodes four *cyd* genes: *cydAB* encode the *bd*-type menaquinol oxidase, whereas *cydDC* encode an ABC-type transporter (reviewed in ref. 9), which is required for cytochrome assembly in *Escherichia coli* (30). These two gene pairs are located 89 bp apart on the *M. tuberculosis* genome. Because it has not been established whether the four genes constitute an operon [they are transcribed as a single transcript in *Bacillus subtilis* (31)], we used probes specific for *cydA* and *cydC* sequences for the RT-PCR measurements. We found that the copy number of the *cydA* transcript was low during acute infection, increased after day 18, peaked on day 30 (7-fold relative to day 15), and dropped back to baseline by day 50 (Fig. 2*D*). Similar, albeit smaller (2.5-fold), changes were observed with the *cydC*-specific probe (Fig. 2*D*).

The down-regulation of both terminal oxidases by day 50 postinfection suggested utilization of alternative electron acceptors in place of O_2 for protonmotive gradient formation and energy conservation. Nitrate reduction is the best-characterized anaerobic respiration pathway of *M. tuberculosis* (32–34): *M. tuberculosis* DNA contains the *narGHJI* operon, which encodes nitrate reductase, and *narK2X*, which encodes the nitrate transporter NarK2 and the ''fused'' inactive nitrate reductase NarX (34). Levels of the *narG* transcript showed little variation throughout infection (Fig. 2*E*). In contrast, levels of the *narK2* transcript increased >10-fold on day 15 relative to day 12 and remained high throughout infection (>20-fold increase on day 100 relative to day 12) (Fig. 2*E*). Thus, the adaptation of *M. tuberculosis* to expression of lung immunity is associated with the transcriptional signature of increased nitrate reduction. As we

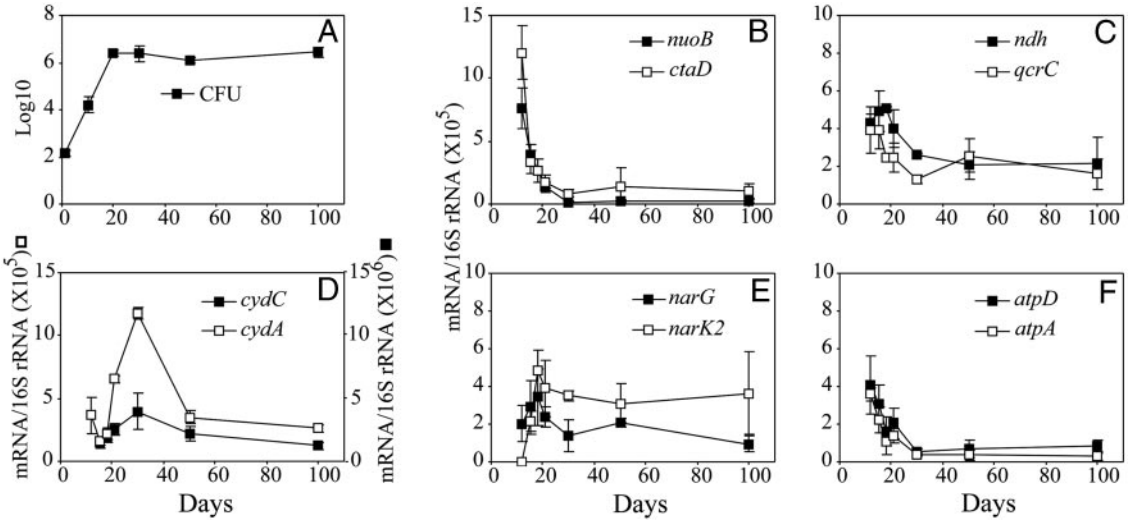

Fig. 2. Transcriptional profiles of selected *M. tuberculosis* genes involved in energy metabolism. (*A*) The course of *M. tuberculosis* infection in the mouse lung. In C57BL/6 mice infected via the respiratory route, tubercle bacilli multiplied exponentially in the lung for ≈20 days (acute infection), and then bacterial replication was inhibited by expression of Th1-mediated immunity (22), causing bacterial numbers to remain stable for the remainder of the infection (chronic infection). (*B–F*) Normalized copy number of bacterial transcripts encoding respiratory and ATP synthesizing enzymes. Lungs were harvested from infected mice at the indicated times, total RNA was extracted, and bacterial transcripts were enumerated by real-time RT-PCR and normalized to 16S rRNA. Normalized copy numbers of *M. tuberculosis* mRNAs were expressed as mean ± SD of data obtained from lungs of three or four mice per time point. In this and subsequent figures, the copy number and fold induction of the transcript detected with the *cydC* probe are lower than that detected with the *cydA* probe. These data do not distinguish whether *cydAB* and *cydDC* are transcribed off two coregulated promoters having different strengths, or whether the *cyd* gene cluster is transcribed as a single polycistronic transcript of ≈6,000 nucleotides that is inefficiently transcribed as full-length molecule.

observed previously (22), transcriptional shifts (as in Fig. 2) preceded control of bacterial infection in the mouse lung, indicating that the transcriptional response takes place before stabilization of the bacterial burden in the lung becomes manifest.

The observed shift to bioenergetically less-efficient respiratory pathways suggested that expression of the bacterial ATP-synthesizing apparatus, which is encoded by the *atpA-H* gene cluster, also would decrease. We found that levels of the *atpD* transcript decreased from day 12 through day 30 (7.5-fold) (Fig. 2*F*). Thereafter, transcript copy numbers remained low. Similar expression levels and transcription patterns were obtained for *atpA* (Fig. 2*F*). Thus, the expression levels of ATP synthesis genes in *M. tuberculosis* are drastically reduced during chronic infection.

A Model of *M. tuberculosis* Respiratory Flexibility During Infection. Based on the *in vivo* data presented above, we propose that *M. tuberculosis* undergoes three successive respiratory states during infection of the mouse lung (Fig. 3). During exponential growth in the mouse lung, *M. tuberculosis* utilizes the respiratory pathway terminating in the aa_3-type oxidase (respiratory state I, Fig. 3). Then expression of Th1-mediated immunity causes activated macrophages to produce NO, which inhibits cellular respiration by competing with O_2 for the binding site on cytochrome *c* oxidase (15, 35). Concurrently, the highly coupled respiratory pathway is strongly down-regulated (up to 70-fold) (Fig. 2*B*), leading to arrest of bacterial replication. Collapse of electron flow, which would disrupt membrane potential and redox homeostasis, is prevented by establishing a new bacterial respiratory state (respiratory state II, Fig. 3) that is characterized by up-regulation of the less energy-efficient cytochrome *bd* oxidase (7-fold) (Fig. 2*D*) and of the nitrate transporter NarK2 (>20-fold) (Fig. 2*E*). Because NarK2 up-regulation reflects increased nitrate reduction in *M. tuberculosis* (34), the transcription profile of respiratory state II suggests that cytochrome *bd* oxidase-dependent aerobic respiration and respiratory nitrate reduction operate in parallel, as described for other microorganisms (8). Due to its high affinity for O_2, cytochrome *bd* oxidase may additionally serve an antioxidant function by scavenging cellular O_2, as seen in many bacteria (9, 36). As cytochrome *bd* oxidase is down-regulated, presumably because of dissipation of the inducing signal as sufficient electron flow and redox balance are restored, respiratory metabolism shifts to nitrate as the preferred terminal electron acceptor (respiratory state III, Fig. 3). A role for nitrate reduction during mouse infection is supported by *in vivo* growth defects observed with *narG* deletion mutants of *Mycobacterium bovis* bacillus Calmette–Guérin (37). Respiratory nitrate reduction contributes greatly to redox balance (8, 38), perhaps reflecting a high requirement for recycling of reducing equivalents when energy is produced primarily from β-oxidation of fatty acids (6). Concurrently, expression levels of ATP synthesis genes decrease (Fig. 2*F*). This reshaping of *M. tuberculosis* energy metabolism is part of the definition of *M. tuberculosis* dormancy.

The changes in energy metabolism in *M. tuberculosis* during infection inferred from transcriptional profiling need independent support. One line of investigation involves use of bacterial mutants to identify genes required for tubercle bacilli to survive the expression of lung immunity, and another involves biochemical assays to determine the nature and extent of the proposed energy metabolism changes. These measurements are best performed with pure bacterial cultures *in vitro*, making it important to establish *in vitro* culture conditions that accurately model the adaptation of *M. tuberculosis* to mouse lung immunity. Data from both lines of investigation are presented below.

Analysis of the *M. tuberculosis cydC* Mutant During Mouse Lung Infection. The transient nature of cytochrome *bd* oxidase up-regulation during the course of lung infection suggests that this enzyme serves an adaptive function in the gradual transition of tubercle bacilli from highly coupled aerobic respiration to less-energy-conserving anaerobic respiration. We examined this possibility by determining the ability of a *M. tuberculosis cydC*

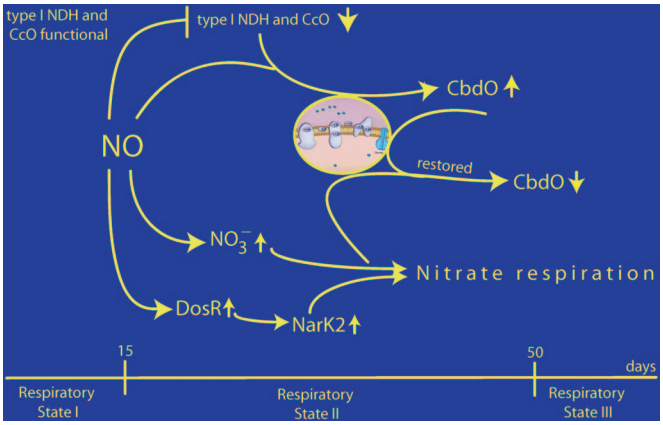

Fig. 3. Respiratory states of *M. tuberculosis* during infection of mouse lung. Presented are events we propose are generated from the high-output production of NO by macrophages activated by Th1-mediated immunity. Respiratory state I: bacteria are actively replicating during acute mouse lung infection, thus requiring high ATP output. This infection phase is characterized by (*i*) the energy-efficient type I NADH dehydrogenase, (*ii*) highly coupled *aa3*-type terminal oxidase (CcO), and (*iii*) low levels of nitrate reductase activity. Respiratory state II: high-output generation of NO blocks the aerobic respiratory pathway terminating with *aa3*-type terminal oxidase and induces bacteriostasis. NO, directly and/or indirectly, causes up-regulation of the *bd*-type terminal oxidase (CbdO). Moreover, NO induces nitrate respiration (*i*) by causing increased formation of nitrate; (*ii*) by causing increased production of the NarK2 nitrate transporter via *dosR*-mediated up-regulation, and (*iii*) by relieving the inhibition of NarK2 activity by O_2. Thus the transient respiratory state II is characterized by (*i*) the nonproton pumping type II NADH dehydrogenase, (*ii*) less efficient *bd*-type terminal oxidase, (*iii*) increased levels of nitrate reduction due to increased availability of nitrate, and (*iv*) reduced levels of ATP synthesis. Moreover, cytochrome *bd* oxidase scavenges O_2 and prevents oxidative damage. Respiratory state III: the pathway terminating with the *bd*-type oxidase is down-regulated in response to the dissipation of the inducing signal. Nitrate respiration is responsible for maintaining redox balance and for energy conservation.

knockout mutant to respond to the expression of lung immunity. When we measured bacterial cfu in the lungs of C57BL/6 mice infected with the *M. tuberculosis* mutant, the mutant complemented with the *cydABDC* gene cluster, and wild-type tubercle bacilli, similar cfu counts were observed 20 days postinfection. Thus the *cydC* mutation did not impair bacillary growth during acute infection (Table 1). In contrast, lung cfu in mice infected with the mutant were 10-fold lower at day 50 relative to day 20 ($\log_{10}$ 6.5 vs. $\log_{10}$ 5.5), indicating a reduced ability to survive the transition from acute to chronic infection. Complementation of the *cydC* mutant with *cydABDC* largely (but not fully) restored bacterial growth. Consistent with a requirement of *cyd* genes during immunity-induced chronic infection, *cydC*-deficient bacteria continued to grow to $\log_{10}$ 7.6 to day 42 in inducible NO synthase-deficient ($NOS2^{-/-}$) mice, at which time the animals died (data not shown). No direct evidence currently exists that the *cydC* mutant strain is impaired in cytochrome *bd* oxidase function. However, in *E. coli*, *cydDC* mutants share all of the phenotypes of *cydAB* mutants (9). Moreover, the adjacent location of *cydAB* and *cydDC* on the *M. tuberculosis* chromosome suggests a functional association between *bd* oxidase and the ABC transporter, as seen in many bacteria (39). Further, the *M. tuberculosis* genome encodes >80 predicted ABC transporters (40), making it reasonable to postulate that the lack of redundancy of *cydDC* function *in vivo* is linked to impaired cytochrome *bd* oxidase function. Thus, the data provided in Table 1 give strong, albeit indirect, evidence that cytochrome *bd* oxidase is required for adaptation of *M. tuberculosis* to conditions generated by expression of lung immunity.

Table 1. cfu enumeration of wild-type and mutant *M. tuberculosis* in lungs of C57BL/6 mice

	Lung cfu ($\log_{10}$)		
M. tuberculosis $H_{37}Rv$	Day 1	Day 20	Day 50
Wild type	2.0 ± 0.05	6.5 ± 0.2	6.7 ± 0.08
cydC::*aph*	1.9 ± 0.03	6.5 ± 0.1	5.5 ± 0.2
cydC::*aph*::pHCYD	2.0 ± 0.1	6.1 ± 0.05	5.8 ± 0.05

C57BL/6 mice at 8–10 weeks of age were infected with ≈100 cfu of *M. tuberculosis* $H_{37}Rv$ WT, *cydC*::*aph*, and *cydC*::*aph* complemented with pHTB-CYD, which carries the *M. tuberculosis cydABDC* gene cluster on an integrative vector (*Materials and Methods*). Lungs were harvested at the indicated days postinfection, homogenized, serially diluted, and plated on enriched Middlebrook 7H11 agar plates for cfu enumeration. Data are expressed as means ± SD obtained from three to four mice per time point.

Transcriptional Response of Respiratory and ATP Synthesis Genes of *M. tuberculosis* to Hypoxia and NO Treatment *in Vitro*. The transcriptional response of tubercle bacilli to expression of mouse lung immunity shares similarities with *M. tuberculosis* cultures undergoing growth arrest caused by gradual O_2 depletion or to treatment with bacteriostatic concentrations of NO (17, 19, 22). To determine how well these *in vitro* culture conditions model *M. tuberculosis* adaptation to mouse lung immunity with regard to respiratory metabolism and ATP synthesis, we measured transcription profiles in these *in vitro* models for the same genes examined *in vivo*.

In the classical Wayne model of gradual oxygen depletion *in vitro* (27, 33), two phases of *M. tuberculosis* growth are described. The first, nonreplicating persistence 1 (NRP-1), initiates when the O_2 level approaches 1% saturation. This microaerobic phase is marked by the arrest of bacterial replication and DNA synthesis. When the dissolved O_2 content of the culture drops to 0.06% saturation, tubercle bacilli shift to an anaerobic stage, NRP-2. We found that the *nuoB* transcript level decreased in both NRP-1 and NRP-2 (3- and 6-fold) relative to aerated mid-log growth, whereas *qcrC* and *ctaD* transcript levels were roughly constant (Fig. 4). Transcript levels for *ndh*, *cydA*, and *cydC* peaked during early NRP-2 (3-fold for *ndh*, 8-fold for *cydA*, and 2.5-fold for *cydC*), with *cydA* increasing even in NRP-1 (4-fold) (Fig. 4). Induction of these transcripts was also detected in microarray-based analyses (23, 41) but, as expected, the magnitude of the change measured by our quantitative RT-PCR assay was greater. Measurements of transcripts involved in nitrate reduction showed that *narG* mRNA remained stable throughout culture, whereas *narK2X* mRNA was strongly up-regulated in both NRP-1 and -2 (≈40- and 120-fold, respectively) (Fig. 4), in accord with previous reports (19, 34). Increased *narK2X* and constitutive *narGHJI* expression provide the transcriptional signature of increased nitrate reduction in *M. tuberculosis* (34). For *atpA* and *atpD* transcripts, copy numbers gradually decreased (3-fold in NRP-2) (Fig. 4).

The same transcripts were measured in cultures of *M. tuberculosis* exposed to NO. Treatment of mid-log aerobically growing bacterial cultures for 30 min with increasing doses of DETA/NO (25–500 μM; see *Materials and Methods*) increased both the number of genes affected and the magnitude of the change in transcript level (Fig. 5). The *narK2X* transcript was up-regulated ≈250-fold in cells treated with 25 μM DETA/NO; no other transcript tested showed copy number changes at the same DETA/NO concentration. Treatment with 100 μM DETA/NO caused a 5-fold decrease of the *nuoB* transcript and a small increase of *ndh* and *cydA* (4- and 3- fold, respectively). Induction of *cydC* became detectable (3.5- to 12-fold) only when treatment was prolonged to 60 min (see Fig. 5 *Inset*). Treatment with 500 μM DETA/NO resulted in a further 25-fold decrease of *nuoB*

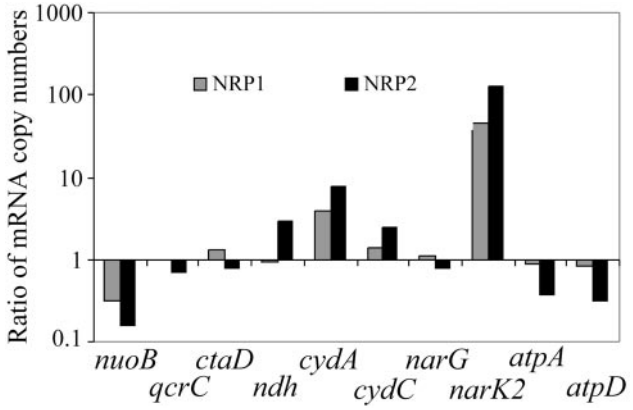

Fig. 4. Normalized copy number of selected *M. tuberculosis* transcripts in liquid cultures exposed to gradual O_2 depletion. *M. tuberculosis* was cultured under conditions of gradual O_2 depletion established by Wayne and Hayes (ref. 27; see *Materials and Methods*). Bacterial RNA was extracted, and transcripts were enumerated by real-time RT-PCR with molecular beacons, as described (22). Levels of transcripts per cell were obtained by dividing mRNA copy number by the corresponding 16S rRNA copy number. Shown are log ratios of normalized mRNA copy numbers determined at 102 h (NRP-1) or 342 h (NRP-2) relative to aerated mid-log cultures. Replicate experiments produced similar results.

and a 4-fold decrease of *qcrC*. Only a minor (2-fold) variation was measured for *ctaD* transcript levels. In contrast, copy numbers of the *ndh* and *cydA* transcripts further increased with the DETA/NO dose, to 6- to 7-fold with 250 μM and to 9-fold with 500 μM DETA/NO (Fig. 5). Although the changes observed in NO-treated cultures for *narK2X*, which is a *dosR*-regulated gene, are in accord with previous reports (17, 21), shifts in the levels of *ndh*, *cydA*, and *cydC* transcripts were not revealed in previous analyses (21, 23, 42), presumably because changes of the scale observed (<10-fold) are readily detected by quantitative RT-PCR but not necessarily by microarray-based transcriptome analysis.

Collectively, the *in vitro* data show that tubercle bacilli treated with NO or under anaerobic incubation (NRP-2) switched from transcription of type I to type II NADH dehydrogenases. This switch represents a significant departure from the *E. coli* paradigm, in which noncoupling dehydrogenases, such as Ndh, are preferentially expressed during aerobic respiration (43), whereas coupling dehydrogenases, such as NuoA-N, are associated with "energy-limited" anaerobic respiratory pathways (44). Moreover, the *bd*-type oxidase genes were up-regulated under both sets of conditions, whereas cytochrome *c* oxidase expression showed a downward tendency in NO-treated cells but not in hypoxic cultures. Overall, these changes were reminiscent of respiratory changes *in vivo*. However, important differences were observed: *ndh* was induced *in vitro* but not *in vivo* (compare Fig. 2*C* with Figs. 3 and 4), and *ctaD* exhibited a large down-regulation *in vivo* but little (NO) or none (hypoxia) *in vitro* (compare Fig. 2*B* with Figs. 3 and 4). Moreover, *cydA* induction was transient in the mouse lung (Fig. 2*D*) but not during hypoxic growth *in vitro* (Fig. 4). Obviously, the situation *in vivo* is multifactorial. For example, down-regulation of *nuoB* and *ctaD* was not as marked in the NO-treated cells as it was *in vivo* (compare Fig. 2*B* with Fig. 5), perhaps because of prolonged exposure to NO *in vivo* or to additional as-yet-unidentified factors. Moreover, even though NO-treated cells show induced *cyd* genes, the induction of cytochrome *bd* oxidase expression seen in mouse lung may also be mediated by proteins sensing integrated signals perhaps derived from changes in respiratory chain efficiency, as previously proposed (23). This latter scenario is supported by the decreased *cydAB* transcript levels by day 50 postinfection, which may result from dissipation of the inducing signal as sufficient electron flow and redox balance are restored by the combined activity of the *bd*-type terminal oxidase and nitrate reductase, as suggested above.

Conclusion

Parallel transcriptional profiling of components of respiratory pathways and of the ATP synthesis apparatus of *M. tuberculosis* during mouse respiratory infection and in two *in vitro* treatments that affect aerobic respiration have identified important similarities consistent with bacterial growth arrest under all three conditions. These data open the way to modification of the *in vitro* conditions tested to better model the transcriptional profiles seen *in vivo*. These observations have the potential of further elucidating the mouse model of infection, which is commonly used for screening new drugs and vaccines against tuberculosis.

The overall implication of the model proposed in Fig. 3 is that respiratory flexibility is an essential component of the adaptation of *M. tuberculosis* to host immunity. This view is supported

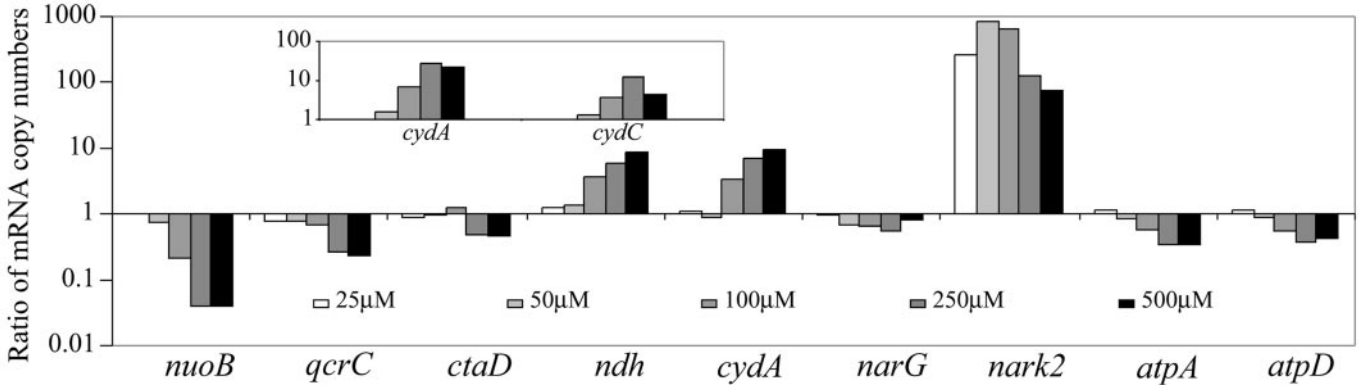

Fig. 5. Normalized copy number of selected *M. tuberculosis* transcripts in liquid cultures exposed to nitric oxide. *M. tuberculosis* cultures were treated with increasing concentrations of the NO donor DETA/NO for 30 and 60 min as described under *Materials and Methods*. Bacterial RNA was extracted, and transcripts were enumerated by real-time RT-PCR with molecular beacons, as described (22). Levels of transcripts per cell were obtained by dividing mRNA copy number by the corresponding 16S rRNA copy number. Shown are log ratios of normalized mRNA copy numbers determined after 30-min treatment relative to aerated mid-log cultures. (*Inset*) Fold changes (3.5- to 12-fold) in the *cydC* transcript in cells treated with 50–500 μM DETA/NO for 60 min; changes (7- to 27-fold) of *cydA* levels under the same conditions are shown for reference. Data for each DETA/NO concentration and treatment duration were obtained in triplicate in three independent cultures.

by the reduced ability of a *cydC* deletion mutant of *M. tuberculosis* to undergo the transition to chronic infection and by *in vivo* growth defects observed with a *narG* deletion mutant of *M. bovis* bacillus Calmette–Guérin (37). Moreover, the proposed role of the *bd*-type terminal oxidase may explain the classic observations relating virulence and hypoxia tolerance in tubercle bacilli (45, 46), because hypoxia tolerance may be a surrogate marker for the pathogen's ability to adapt to conditions created by host immunity. If our model is correct, it will lead to new targets for drugs and vaccines against tuberculosis.

We thank Lynn Ryan and Ron LaCourse (Trudeau Institute) for mouse infections. We are also grateful to Karl Drlica, Carol Lusty, David Perlin, and Larry Wayne for stimulating discussions and critical reading of this manuscript. Special thanks go to Harvey Penefsky for his help in highlighting the significance of the findings and their implications in the biochemistry of the *M. tuberculosis*-infected lung. V.M. and B.D.K. also thank Harvey Rubin for stimulating their interest in the field of *M. tuberculosis* respiration. This work was supported by grants from the Medical Research Services of the U.S. Department of Veterans Affairs (to C.S.), the Medical Research Council of South Africa and the Howard Hughes Medical Institute (International Scholars Grant) (to V.M.), the Futura Foundation (to M.L.G.), and National Institutes of Health [Grants AI-37844 and AI-059557 (to R.J.N.); Grant AI-43420 (to Harvey Rubin, supporting work in V.M.'s laboratory); and AI-36989 (to M.L.G.)].

1. Segal, W. (1984) in *The Mycobacteria, A Sourcebook*, eds. Kubica, G. P. & Wayne, L. G. (Dekker, New York), pp. 547–573.
2. Wayne, L. G. (1994) *Eur. J. Clin. Microbiol. Infect. Dis.* **13,** 908–914.
3. Honer zu Bentrup, K. & Russell, D. G. (2001) *Trends Microbiol.* **9,** 597–605.
4. Stewart, G. R., Robertson, B. D. & Young, D. B. (2003) *Nat. Rev. Microbiol.* **1,** 97–105.
5. Monack, D. M., Mueller, A. & Falkow, S. (2004) *Nat. Rev. Microbiol.* **2,** 747–765.
6. McKinney, J. D., Honer zu Bentrup, K., Munoz-Elias, E. J., Miczak, A., Chen, B., Chan, W. T., Swenson, D., Sacchettini, J. C., Jacobs, W. R., Jr., & Russell, D. G. (2000) *Nature* **406,** 735–738.
7. Segal, W. & Bloch, H. (1956) *Infect. Immun.* **72,** 132–141.
8. Richardson, D. J. (2000) *Microbiology* **146,** 551–571.
9. Poole, R. K. & Cook, G. M. (2000) *Adv. Microb. Physiol.* **43,** 165–224.
10. Mogues, T., Goodrich, M. E., Ryan, L., LaCourse, R. & North, R. J. (2001) *J. Exp. Med.* **193,** 271–280.
11. Rees, R. & D'Arcy Hart, P. (1961) *Br. J. Exp. Pathol.* **42,** 83–88.
12. Munoz-Elias, E. J., Timm, J., Botha, T., Chan, W. T., Gomez, J. E. & McKinney, J. D. (2005) *Infect. Immun.* **73,** 546–551.
13. Flynn, J. L. & Chan, J. (2001) *Annu. Rev. Immunol.* **19,** 93–129.
14. North, R. J. & Jung, Y. J. (2004) *Annu. Rev. Immunol.* **22,** 599–623.
15. Brunori, M., Giuffre, A., Forte, E., Mastronicola, D., Barone, M. C. & Sarti, P. (2004) *Biochim. Biophys. Acta* **1655,** 365–371.
16. MacMicking, J., Xie, Q. W. & Nathan, C. (1997) *Annu. Rev. Immunol.* **15,** 323–350.
17. Voskuil, M. I., Schnappinger, D., Visconti, K. C., Harrell, M. I., Dolganov, G. M., Sherman, D. R. & Schoolnik, G. K. (2003) *J. Exp. Med.* **198,** 705–713.
18. Dasgupta, N., Kapur, V., Singh, K. K., Das, T. K., Sachdeva, S., Jyothisri, K. & Tyagi, J. S. (2000) *Tuber. Lung Dis.* **80,** 141–159.
19. Sherman, D. R., Voskuil, M., Schnappinger, D., Liao, R., Harrell, M. I. & Schoolnik, G. K. (2001) *Proc. Natl. Acad. Sci. USA* **98,** 7534–7539.
20. Roberts, D. M., Liao, R. P., Wisedchaisri, G., Hol, W. G. & Sherman, D. R. (2004) *J. Biol. Chem.* **279,** 23082–23087.
21. Schnappinger, D., Ehrt, S., Voskuil, M. I., Liu, Y., Mangan, J. A., Monahan, I. M., Dolganov, G., Efron, B., Butcher, P. D., Nathan, C., *et al.* (2003) *J. Exp. Med.* **198,** 693–704.
22. Shi, L., Jung, Y. J., Tyagi, S., Gennaro, M. L. & North, R. J. (2003) *Proc. Natl. Acad. Sci. USA* **100,** 241–246.
23. Boshoff, H. I., Myers, T. G., Copp, B. R., McNeil, M. R., Wilson, M. A. & Barry, C. E., 3rd (2004) *J. Biol. Chem.* **279,** 40174–40184.
24. Andries, K., Verhasselt, P., Guillemont, J., Gohlmann, H. W., Neefs, J. M., Winkler, H., Van Gestel, J., Timmerman, P., Zhu, M., Lee, E., *et al.* (2005) *Science* **307,** 223–227.
25. Weinstein, E. A., Yano, T., Li, L. S., Avarbock, D., Avarbock, A., Helm, D., McColm, A. A., Duncan, K., Lonsdale, J. T. & Rubin, H. (2005) *Proc. Natl. Acad. Sci. USA* **102,** 4548–4553.
26. Dunn, P. L. & North, R. J. (1995) *Infect. Immun.* **63,** 3428–3437.
27. Wayne, L. G. & Hayes, L. G. (1996) *Infect. Immun.* **64,** 2062–2069.
28. Desjardin, L. E., Hayes, L. G., Sohaskey, C. D., Wayne, L. G. & Eisenach, K. D. (2001) *J. Bacteriol.* **183,** 5311–5316.
29. Kana, B. D., Weinstein, E. A., Avarbock, D., Dawes, S. S., Rubin, H. & Mizrahi, V. (2001) *J. Bacteriol.* **183,** 7076–7086.
30. Cruz-Ramos, H., Cook, G. M., Wu, G., Cleeter, M. W. & Poole, R. K. (2004) *Microbiology* **150,** 3415–3427.
31. Winstedt, L., Yoshida, K., Fujita, Y. & von Wachenfeldt, C. (1998) *J. Bacteriol.* **180,** 6571–6580.
32. Wayne, L. G. & Hayes, L. G. (1998) *Tuber. Lung Dis.* **79,** 127–132.
33. Wayne, L. G. & Sohaskey, C. D. (2001) *Annu. Rev. Microbiol.* **55,** 139–163.
34. Sohaskey, C. D. & Wayne, L. G. (2003) *J. Bacteriol.* **185,** 7247–7256.
35. Shiva, S. & Darley-Usmar, V. M. (2003) *IUBMB Life* **55,** 585–590.
36. Rezaiki, L., Cesselin, B., Yamamoto, Y., Vido, K., van West, E., Gaudu, P. & Gruss, A. (2004) *Mol. Microbiol.* **53,** 1331–1342.
37. Weber, I., Fritz, C., Ruttkowski, S., Kreft, A. & Bange, F. C. (2000) *Mol. Microbiol.* **35,** 1017–1025.
38. Moreno-Vivian, C., Cabello, P., Martinez-Luque, M., Blasco, R. & Castillo, F. (1999) *J. Bacteriol.* **181,** 6573–6584.
39. Binet, R., Letoffe, S., Ghigo, J. M., Delepelaire, P. & Wandersman, C. (1997) *Gene* **192,** 7–11.
40. Braibant, M., Gilot, P. & Content, J. (2000) *FEMS Microbiol. Rev.* **24,** 449–467.
41. Voskuil, M. I., Visconti, K. C. & Schoolnik, G. K. (2004) *Tuberculosis* **84,** 218–227.
42. Ohno, H., Zhu, G., Mohan, V. P., Chu, D., Kohno, S., Jacobs, W. R., Jr. & Chan, J. (2003) *Cell Microbiol.* **5,** 637–648.
43. Green, J. & Guest, J. R. (1994) *Mol. Microbiol.* **12,** 433–444.
44. Unden, G. & Bongaerts, J. (1997) *Biochim. Biophys. Acta* **1320,** 217–234.
45. Guy, L. R., Raffel, S. & Clifton, C. E. (1954) *J. Infect. Dis.* **94,** 99–106.
46. Heplar, J. Q., Clifton, C. E., Raffel, S. & Futrelle, C. M. (1954) *J. Infect. Dis.* **94,** 90–98.
47. Babcock, G. T. (1999) *Proc. Natl. Acad. Sci. USA* **96,** 12971–12973.
48. Niebisch, A. & Bott, M. (2003) *J. Biol. Chem.* **278,** 4339–4346.
49. Cole, S. T., Brosch, R., Parkhill, J., Garnier, T., Churcher, C., Harris, D., Gordon, S. V., Eiglmeier, K., Gas, S., Barry, C. E., 3rd, *et al.* (1998) *Nature* **393,** 537–544.